HIV disrupts CD34^{+} progenitors involved in T-cell differentiation

*Tetsuo Tsukamoto [1, 2, 3]

[1] The Kirby Institute for infection and immunity in society, University of New South Wales, Sydney, Australia

[2] Center for AIDS Research, Kumamoto University, Kumamoto, Japan

[3] Department of Immunology, Kindai University Faculty of Medicine, Osaka, Japan

*Corresponding author mailing address: Department of Immunology, Kindai University Faculty of Medicine, 377-2 Onohigashi, Osakasayama-shi, 589-8511 Osaka, Japan

Telephone: +81 72 366 0221

Fax: +81 72 367 7660

Email: ttsukamoto@med.kindai.ac.jp

Summary

HIV-1 causes the loss of $CD4^+$ T cells via depletion or impairment of their production. The latter involves infection of thymocytes, but the involvement of other cells including haematopoietic $CD34^+$ cells remains unclear even though HIV-positive patients frequently manifest myelosuppression. In this study, we utilised the OP9-DL1 coculture system, which supports in vitro T-lineage differentiation of human haematopoietic stem/progenitor cells. Cord-derived $CD34^+$ cells were infected with CXCR4-tropic HIV-1_{NL4-3} and cocultured. HIV-infected cocultures exhibited sustained viral replication for 5 weeks, as well as reduced $CD4^+$ T-cell growth at weeks 3–5. We further revealed that $CD34^+CD7^+CXCR4^+$ cells can be quickly depleted as early as in 1 week after infection of the subset, and this was accompanied by the emergence of $CD34^+CD7^+CD4^+$ cells. These results indicate that CXCR4-tropic HIV-1 strains may disrupt $CD34^+CD7^+$ lymphoid progenitor cell pools, presumably leading to impaired T-cell production potential.

Keywords

human immunodeficiency virus, acquired immunodeficiency syndrome, haematopoietic stem/progenitor cells, C-X-C chemokine receptor type 4

38 **Introduction**

39

40 Human immunodeficiency virus (HIV) infection is associated with
41 haematological changes [1]. Antiretroviral therapy is effective in controlling viremia
42 and treating AIDS. However, some patients do not experience sufficient T-cell
43 immune restoration despite being aviremic during treatment [2]. HIV-infected patients
44 may display decreased thymopoiesis [3]. Thymic dysfunction occurs during HIV
45 infection, and it is associated with rapid progression in infants with prenatal HIV
46 infection [4]. A previous report tested coculture of $CD34^+$ and fetal thymic epithelial
47 cells in the presence or absence of HIV-1, observing that infection led to the
48 inhibition of thymocyte maturation at early stages ($CD44^+CD25^-CD3^-$) [5].
49 Pancytopenia may occur as a result of bone marrow abnormalities in HIV-infected
50 individuals [6,7]. A previous study revealed depletion of $CD34^+CD4^+$ cells in bone
51 marrow from HIV-infected patients. However, the study failed to uncover evidence of
52 HIV infection of these cells [8].

53 The thymopoiesis environment can be mimicked in vitro using the OP9-DL1 or
54 OP9-DL4 cell line. These cell lines were derived from the OP9 mouse stromal cell
55 line via transduction with a notch ligand called delta-like 1 (DL1) or DL4 [9,10]. The
56 ability of OP9-DL1 cells to support thymopoiesis in vitro was first demonstrated in
57 coculture with mouse cells [9]. The cell line is also known to support the differentiation
58 of human $CD34^+$ haematopoietic stem/progenitor cells (HSPCs) into thymocytes and
59 T cells [11]. There is evidence that OP9-DL1 cells produce stromal derived factor-1
60 (SDF-1, also known as CXCL12), a ligand for CXCR4 [12]. Although OP9-DL4 cells
61 can induce differentiation into both specific myeloid cells and T-lineage cells, OP9-
62 DL1 cells only permit the differentiation of T-lineage cells while inhibiting B cells

63 and myeloid cells [13]. Thus, the OP9-DL1 coculture system is used to investigate
64 events associated with T-lineage differentiation.

65 CXCR4 and CCR5 are common coreceptors for HIV-1 [14]. Control of CCR5-
66 tropic strains of HIV-1 is usually considered a better correlate of good clinical
67 outcomes than control of CXCR4-tropic HIV-1 strains [15]. This is due to the fact that
68 memory $CD4^+$ T cells express higher levels of CCR5, thus making them susceptible
69 to CCR5-tropic HIV infection and subsequent depletion [16]. Consequently, CCR5 may
70 appear to be more closely involved in the immunopathogenesis of HIV infection than
71 CXCR4 [17]. Conversely, the biological functions of CXCR4 have been well
72 documented in fields such as developmental biology and haematology. CXCR4
73 interacts with SDF-1 and allows CXCR4-expressing cells to home to loci in which
74 SDF-1 is highly expressed [18]. SDF-1 and CXCR4 are essential in human stem cell
75 homing and repopulation of the host with differentiated haematopoietic cells [19,20].
76 SDF-1 is also produced by thymic epithelial cells, and it plays an important role in
77 migration of immature progenitors in the thymus [21].

78 Therefore, it may be important to better understand the influence of CXCR4-
79 tropic HIV-1 infection on CXCR4-associated biological events including
80 haematopoiesis and T-cell development. A prior study sought to clarify the effect of
81 CXCR4-tropic simian-human immunodeficiency virus infection on T-lineage cell
82 production in the thymi of newborn rhesus macaques [22]. However, it is not realistic to
83 closely follow in vivo bone marrow/thymus events in HIV-infected individuals.
84 Instead, humanised mouse models can be beneficial for this purpose [23,24]. Moreover,
85 an easy-to-use ex-vivo model may be helpful for closely monitoring the
86 differentiation of HSPCs into T-lineage cells in the presence of HIV-1. The present

87 study aimed to determine the in vitro fate of $CD34^+$ progenitor cells and derivatives

88 exposed to HIV-1 using the OP9-DL1 coculture system.

89

90

91 **Results**

92

93 *Persistent HIV-1 infection observed in OP9-DL1 cocultures with cord-derived CD34$^+$*
94 *cells*

95 Two separate in vitro experiments were performed in the study. The data for
96 experiment 1 (long coculture) are shown in Figs. 1–3 and Extended Data Figs. 1–5.
97 To follow the in vitro fate of HIV–pre-exposed CD34$^+$ cells and derivatives for
98 several weeks, we infected primary human umbilical cord-derived CD34$^+$ cells with
99 HIV-1. These cells were partially CD4$^+$ and/or CXCR4$^+$ before infection (Extended
100 Data Fig. 1A). Cells were seeded in 48-well plates and exposed to 200 ng (p24) of
101 HIV-1$_{NL4-3}$. Following centrifugation and overnight incubation in the presence of
102 HIV-1, the cells were cocultured with OP9-DL1 cells (Fig. 1A). After a week of
103 coculture, intracellular HIV-1 p24 was detected in both CD34$^+$ and CD34$^-$ cells (Fig.
104 1B). HIV infection was further examined via magnetic bead separation of CD34$^+$ and
105 CD34$^-$ cells followed by DNA extraction and detection of HIV-1 *gag* DNA using
106 PCR (Extended Data Fig. 1B). The HIV-infected samples displayed persistent HIV-1
107 p24 expression in 0.1–1.7% of the total cocultured human cells (Fig. 1C, Extended
108 Data Fig. 1C–G). A correlation was found between intracellular HIV-1 p24$^+$ cell
109 counts and supernatant HIV-1 p24 concentrations (Extended Fig. 1E).

110

111 *The dynamics of CD4$^+$ cells in OP9-DL1 cocultures with HIV–pre-exposed CD34$^+$*
112 *cells*

113 The influence of HIV pre-exposure of CD34$^+$ cells on post-coculture events was
114 analysed by flow cytometry weekly until week 5. CD19$^+$, CD20$^+$ or CD33$^+$ cells were

115 not detected in the samples tested (data not shown). HIV-infected cocultures had
116 significantly lower whole cell counts at weeks 3, 4 and 5 post-coculture than
117 uninfected cocultures (Extended Data Fig. 2A), demonstrating reduced cell growth in
118 the presence of HIV-1. Similarly, the $CD4^+CD8^+$ and $CD4^+CD8^+CXCR4^+$ cell counts
119 were significantly smaller in HIV^+ cocultures than in HIV^- cocultures at week 3
120 (Extended Data Fig. 2B–D). When $CD34^-$ cells were gated and analysed for CD7 and
121 CD4 expression (Fig. 2A), the $CD34^-CD7^+CD4^+$ cell counts were not significantly
122 different between HIV-infected and uninfected samples (Fig. 2B). By contrast, there
123 was a notable decline in $CD34^-CD7^-CD4^+$ cell counts in HIV^+ samples compared to
124 those in HIV^- samples at week 3 (Fig. 2C). Further analysis of $CD34^-$ cells revealed
125 that the $CD7^+CD4^+$ cells contained CD4/CD8 double-positive cells and $CD3^+CD4^+$
126 cells, whereas the $CD7^-CD4^+$ cells were mostly $CD3^+CD4^+$ cells (Extended Data Fig.
127 3). In the analysis of $CD34^-CXCR4^+$, $CD34^-CD7^+CXCR4^+$ and $CD34^-CD7^-CXCR4^+$
128 cells, the $CD34^-CD7^-CXCR4^+$ cells exhibited the greatest growth impairment
129 following HIV-1 infection (Extended Data Fig. 4).
130
131 *The dynamics of $CD34^+$ cells in OP9-DL1 cocultures with HIV–pre-exposed $CD34^+$*
132 *cells*
133 HIV infection of $CD34^+$ cells was detected by intracellular $p24^+$ staining
134 followed by flow cytometric analysis (Fig. 3A–B, Extended Data Fig. 5A–D).
135 $p24^+CD34^+$ cells failed to grow by week 2 (Fig. 3A), in contrast to the rapid growth of
136 $p24^+$ cells at this time point (Fig. 1C). $p24^+CD34^+CD7^+$ cell counts increased at weeks
137 2 and 3 (Fig. 3B) in association with a low average $CD34^+CD7^+$ cell count in week 1
138 after infection and a rapid increase in week 2 (Fig. 3C). Then, $CD34^+$ cell dynamics in
139 HIV^+ samples were compared with those in HIV^- samples (Fig. 3C-D, Extended Data

140 Fig. 5E–G). There were nonsignificant differences in $CD34^+CD7^+$ cell counts
141 between HIV^+ and HIV^- cocultures (Fig. 3C). The difference in the average
142 frequencies of $CD34^+CD7^+$ cells was greatest at week 3 (Fig. 3C). However, the
143 average $CD34^+CD7^+CXCR4^+$ cell count in HIV^+ cocultures versus that in HIV^-
144 cocultures exhibited the greatest difference at week 2 (Fig. 3D). Therefore,
145 $CD34^+CD7^+CXCR4^+$ cells may be affected by HIV-1 earlier than the entire
146 $CD34^+CD7^+$ cell population or cells of other phenotypes.
147
148 *HIV-1_{NL4-3} infection of HSPC-derived cells after 4–6 weeks of coculture with OP9-*
149 *DL1 cells*
150 To better describe the effect of HIV infection on the short-term dynamics of
151 $CD34^+$ cells, experiment 2 was performed (short coculture, n = 12, Fig. 4A). The
152 experiment 2 results are shown in Figs. 4–6, Extended Data Figs. 6–8 and Extended
153 Data Tables 1–2. Briefly, coculture of OP9-DL1 cells with HIV-uninfected cord-
154 derived $CD34^+$ cells for 4–6 weeks produced a mixture of cells with different
155 phenotypes as determined by the expression of CD34, CD4, CD8, CD7 and CXCR4
156 (Figs. 1–3, Extended Data Figs. 1–5). CD4 expression levels in $CD34^+$ cells before
157 infection were lower than those in $CD34^-$ cells (Fig. 4B). Cells were then harvested
158 and infected with HIV-1_{NL4-3} following the procedures for HIV infection of $CD34^+$
159 cells (Fig. 1A). The infected cells were cocultured again with a new OP9-DL1
160 monolayer and further incubated for 1 week (Fig. 4A). One week after infection, HIV
161 replication was detected in all HIV-infected samples (Fig. 4C). The majority of HIV-1
162 $p24^+$ cells were $CD34^-$ (Fig. 4C, Extended Data Fig. 6). The majority of $p24^+CD34^+$
163 cells were $CD7^+$ (Fig. 4C, Extended Data Table 1).
164

165 *Partial loss of CD34$^+$CD7$^+$CXCR4$^+$ cells after HIV-1$_{NL4-3}$ infection of OP9-DL1–*
166 *cocultured cells*

167 The phenotypes of the cells in experiment 2 (short coculture) were analysed 1
168 week after infection (Fig. 5, Extended Data Fig. 7, Extended Data Table 2). The
169 whole cell counts were obtained using parts of the tested batches, with no significant
170 differences noted between HIV$^+$ and HIV$^-$ samples (n = 4, p = 0.5000, Extended Data
171 Table 2). The frequencies of CD4$^+$CD8$^+$, CD34$^+$ and CD34$^+$CD7$^+$ cells were not
172 significantly different between HIV$^+$ and HIV$^-$ cocultures (Extended Data Fig. 7).
173 Regarding CXCR4 expression levels in different subsets, the frequencies of
174 CD34$^+$CD7$^+$CXCR4$^+$ cells in HIV$^+$ samples were significantly reduced compared to
175 those in HIV$^-$ samples (Fig. 5A and C middle). This may be in accordance with the
176 results in Fig. 3D in which the growth of CD34$^+$CD7$^+$CXCR4$^+$ cells slowed earlier (at
177 week 2) than those of other phenotypes (at week 3).

178

179 *Increased number of CD34$^+$CD7$^+$CD4$^+$ cells after HIV-1$_{NL4-3}$ infection of OP9-DL1–*
180 *cocultured cells*

181 Figure 5 indicates the distinct dynamics of CD34$^+$CD7$^+$CXCR4$^+$ cells in the
182 presence of HIV-1. For increased clarity, CD34$^+$CD7$^+$ cells were further analysed for
183 CD4 expression (Fig. 6, Extended Data Fig. 8). Surprisingly, HIV-infected samples
184 had higher frequencies of CD34$^+$CD7$^+$CD4$^+$CXCR4$^+$ cells than uninfected samples
185 (Fig. 6A and B). These cells were found to be partially HIV p24$^+$ after carefully
186 adjusting the compensation matrices of the flow cytometry data (Fig. 6A and C). One
187 of nine batches was selected for further analyses of CD34$^+$CD7$^+$CD4$^+$ cells. Both the
188 frequencies and CD4 fluorescence intensities of CD34$^+$CD7$^+$CD4$^+$ cells were higher
189 in HIV$^+$ samples than in HIV$^-$ samples (Extended Fig. 8B), implying the emergence

190 of $CD34^{+}CD7^{+}CD4^{hi}$ cells. In addition, the frequencies of $CD34^{+}CD7^{+}CD4^{+}CXCR4^{+}$

191 cells were correlated with those of $p24^{+}$ cells (Fig. 6D).

192 **Discussion**

193

194 Regarding the dynamics of $CD34^+$ cells in HIV-infected individuals, there has
195 been a debate regarding whether HSPCs comprise an unignorable viral reservoir [25].
196 There is also a possibility of modified turnover of HSPCs through HIV infection and
197 depletion of $CD4^+$ cells. For example, HIV infection commonly manifests as bone
198 marrow abnormalities [26]. Some patients fail to exhibit $CD4^+$ T-cell recovery even
199 after effective antiretroviral therapy, thus being termed immunological nonresponders.
200 Such immunological nonresponsiveness can be associated with immune activation
201 and/or bone marrow impairment [27,28]. To approach these problems, the present study
202 revealed a method for utilising the OP9-DL1 coculture system, which enables in vitro
203 follow-up of the early events in T-cell differentiation such as lymphoid progenitor cell
204 generation that normally occur in the bone marrow as well as $CD4^+$ thymocyte
205 differentiation in the thymus. The events observed in the cocultures of OP9-DL1 and
206 human $CD34^+$ cells are likely to involve interactions between SDF-1 and CXCR4, as
207 mouse SDF-1 expressed by OP9-DL1 cells has high amino acid sequence identity
208 with human SDF-1 [29]. The observation is in accordance with previous reports
209 illustrating that the SDF-1/CXCR4 pair is crucially involved in the homing and
210 repopulation of HSPCs in specific bone marrow niches [30] and the entire T-cell
211 developmental process in the thymus [21,31]. It has been reported that HSPCs and
212 thymocytes express CXCR4, but their CCR5 expression is limited [32]. Another report
213 indicated that HIV utilises CXCR4 when it infects multipotent progenitor cells [33].
214 CXCR4-tropic HIV strains might contribute to pathogenesis by interfering with
215 haematopoiesis and/or lymphopoiesis [34-36], although the underlying mechanisms are
216 yet to be unveiled.

217 The present results provide insights into the impact of HIV-1 on T-lineage
218 differentiation of haematopoietic progenitor cells. In experiment 1 (long coculture),
219 HIV-infected samples exhibited similar $CD4^+$ cell production rates as uninfected
220 samples at weeks 1 and 2 but reduced $CD4^+$ cell production rates from week 3 to
221 week 5 (Fig. 2). This was most clearly observed with the dynamics of
222 $CD34^-CD7^-CD4^+$ cells (Fig. 2C) that were mostly $CD3^+$ T cells (Extended Data Fig.
223 3). It is unclear how the reduction of cell growth at week 3 after infection was so
224 accurately reproduced in the 12 samples tested (Fig. 2C, individual data not shown).
225 However, in the subsequent analyses of $CD34^+$ cells, the growth rates of
226 $CD34^+CD7^+CXCR4^+$ cells tended to fall as early as week 2 (Fig. 3D). This was
227 observed in 7/12 samples tested (data not shown), and the decline occurred earlier
228 than the reduction in $CD34^-CD7^-CD4^+$ cell counts (week 3). Because $CD34^+CD7^+$
229 cells represent lymphoid progenitor cells [37], their involvement in defining the
230 production rates of $CD4^+$ cells may be speculated.

231 Subsequently, experiment 2 (short coculture, Figs. 4–6) was conducted to
232 examine the effects of HIV-1 on the short-term dynamics of T-lineage cells including
233 $CD34^+$ progenitors. HIV-1 infection resulted in significant decreases of the frequency
234 of $CD34^+CD7^+CXCR4^+$ cells 1 week after infection (Fig. 5B right), which may be
235 consistent with the results of experiment 1 (Fig. 3D). Because of the limitation of the
236 present study, the fate of the lost $CD34^+CD7^+CXCR4^+$ cells in the HIV^+ cocultures is
237 unknown. The differentiation capacity of the remaining $CD34^+CD7^+CXCR4^+$ cells
238 also remains untested. Interestingly, a recent article reported that bone marrow $CD34^+$
239 progenitor cells from HIV-infected patients exhibit impaired T-cell differentiation
240 potential [38], which was related to proinflammatory cytokines. Cytokine analyses may
241 be applicable to the coculture assays we established in the present study.

242 The $CD34^+CD7^+$ progenitors were further analysed to better understand their
243 association with HIV-1 infection. Interestingly, the frequencies of $CD34^+CD7^+CD4^+$
244 cells were elevated in HIV-infected samples compared to those in uninfected samples
245 (Fig. 6, Extended Data Fig. 8). In addition, $CD34^+CD7^+CD4^+$ cells were found to be
246 partially HIV $p24^+$ (Fig. 6A and C). It may be fascinating to interpret the results as
247 CD4 upregulation following HIV infection, thereby driving the differentiation of T-
248 lineage precursor cells. However, caution may be necessary because exclusion of
249 possible CD34 upregulation in the infected $CD4^+$ cells was not confirmed in this
250 study (Extended Data Fig. 8), although the flow cytometry data did not indicate
251 correlations between HIV p24 expression and CD34 upregulation in $CD34^{low}$ cells
252 (data not shown). Further studies may be designed to test shorter coculture periods
253 than 1 week and/or investigate the association of HIV-1 infection with factors that
254 regulate the expression of CD3, CD4, CD7 and CD34. Such analyses will also help
255 better clarify the debate on the issues of $CD34^+$ viral reservoirs [25].

256 The findings in this article highlight the potential of anti-HIV treatments such as
257 gene therapy using $CD34^+$ HSPCs followed by transplantation because in this manner,
258 all haematopoietic events in the host can be protected against HIV infection by the
259 gene products even in the absence of effective immune responses [39]. The problem is
260 that although CCR5 may be considered a reasonable target for knockout or
261 knockdown to prevent infection by CCR5-tropic HIV strains, CXCR4 expression
262 should not be altered in HSPCs because of the essential biological functions of the
263 molecule [40]. Therefore, instead of modulating CXCR4 expression, anti-HIV
264 modalities targeting an HIV gene or component may be desirable for protecting
265 haematopoietic cells including T-lineage cells from CXCR4-tropic HIV infection [41].

266 In summary, the results of the long/short coculture of human $CD34^+$ cells and
267 derivatives with OP9-DL1 cells in the presence of HIV-1 indicate that the dynamics
268 of $CD34^+CD7^+$ lymphoid progenitors may be affected more quickly by HIV-1 than
269 $CD34^-CD4^+$ thymocytes and T cells despite the lower susceptibility of $CD34^+CD7^+$
270 cells to HIV-1 infection as suggested by their lower CD4 expression levels. Further
271 studies may be designed to elucidate the underling mechanisms. In addition, the
272 preceding reduction of $CD34^+CD7^+CXCR4^+$ cell growth at week 2 followed by the
273 reduction of $CD34^-CD4^+$ cell growth at week 3 in the HIV^+ cocultures may illustrate
274 the mechanism by which reduced sizes of progenitor cell pools may decelerate the
275 production of T cells in HIV-infected patients (Extended Data Fig. 9). In HIV-
276 infected patients, this may occur in combination with different mechanisms of $CD4^+$
277 T-cell depletion including direct cytopathic effects, apoptosis and antigen-specific
278 immunological mechanisms [42,43].
279

280 **Methods**

281

282 **Virus stocks.** Stocks of HIV-1_{NL4-3} were produced via transfection of 293T cells with
283 the molecular clone DNA pNL4-3 [44]. After transfection, the culture supernatant was
284 collected, and viral loads were determined using an HIV p24 enzyme-linked
285 immunosorbent assay (ELISA) kit (ZeptoMetrix, NY, USA).

286

287 **Cells.** Umbilical cord blood samples were collected at Fukuda Hospital, Kumamoto,
288 Japan after obtaining informed consent. Cord blood mononuclear cells were isolated
289 using Pancoll (PAN-Biotech GmbH, Aidenbach, Germany) and centrifugation at 800
290 rpm for 20 min. $CD34^+$ cells were labelled and selected using human CD34
291 microbeads and LS columns (Miltenyi Biotec, NSW, Australia). The purity constantly
292 exceeded 92%. The OP9-DL1 cell line was generated via transduction of the OP9 cell
293 line (ATCC CRL-2749) with human DL1. The cell line was maintained in α-MEM
294 medium (Wako Pure Chemical Industries, Osaka, Japan) supplemented with 10% heat
295 inactivated fetal bovine serum (FBS, GE Healthcare, Tokyo, Japan).

296

297 **Antibodies.** Anti-human CD8 Brilliant Violet (BV) 510 (clone RPA-T8), anti-human
298 CD3 PE-Cy7 (clone UCHT1) and anti-human CD34 APC (clone 8G12) were
299 purchased from BD Biosciences (Tokyo, Japan). Anti-human CD4 PE-Cy7 (clone
300 OKT4), anti-human CD4 PerCP-Cy5.5 (clone OKT4) and anti-human CXCR4
301 BV421 (clone 12G5) were purchased from BioLegend (Tokyo, Japan). Anti-human
302 CD3 ECD (clone UCHT1) and anti-HIV-1 p24 PE (clone FH190-1-1, also known as
303 KC57 RD1) were purchased from Beckman Coulter (Tokyo, Japan). Anti-human CD7
304 FITC (clone CD7-6B7) was purchased from CALTAG Laboratories (CA, USA),

305

306 **Coculture of human cells with OP9-DL1.** The OP9-DL1 coculture experiment was
307 performed following a previously published protocol with modifications [45]. Briefly, 2
308 × 10^5 HIV-infected or uninfected cord-derived $CD34^+$ cells were seeded in a 6-well
309 plate (Corning, Tokyo, Japan) containing a OP9-DL1 monolayer. The coculture was
310 maintained for 5 weeks in α-MEM medium supplemented with 20% heat inactivated
311 FBS, 5 ng/mL recombinant human FMS-like tyrosine kinase 3 ligand (R&D Systems,
312 MN, USA) and 5 ng/mL recombinant human interleukin 7 (Miltenyi Biotec). Cells
313 were passaged weekly with vigorous pipetting and filtering through a 70-μm
314 membrane and cocultured again with a fresh monolayer of OP9-DL1 cells. A portion
315 of the collected cells was analysed by flow cytometry.

316

317 **HIV infection.** The method for in vitro HIV infection of $CD34^+$ cells was described
318 previously [46]. To infect primary cord-derived $CD34^+$ cells with HIV-1_{NL4-3}, a 48-well
319 plate (Corning) was treated overnight with RetroNectin (Takara Bio, Kusatsu, Japan)
320 at a concentration of 10 μg/mL. $CD34^+$ cells were re-suspended in the OP9-DL1
321 medium, seeded at 2 × 10^5 per well in the coated plate and infected with 200 ng (p24)
322 of HIV-1_{NL4-3} using spinoculation at 1200 × *g* at 34°C for 30 min. Cells were further
323 cultured overnight and cocultured in a 6-well plate with a fresh monolayer of OP9-
324 DL1 cells. For HIV infection of OP9-cocultured human cells, the cell concentration
325 was modified to 5 × 10^5 per well.

326

327 **Flow cytometry.** Surface and intracellular antigen expression was analysed using a
328 FACS LSR II (BD Biosciences), FACS Diva v6.0 software (BD Biosciences) and
329 FlowJo v10.3 software (FlowJo, OR, USA). Dead cells were discriminated using

330 Live/Dead Fixable Near-IR Dead Cell Stains (Thermo Fisher Scientific, VIC,
331 Australia). Live cells were further gated to exclude doublets from the analysis by
332 plotting FSC-W and FSC-A.
333
334 **PCR analysis of HIV DNA.** Cellular DNA was extracted using a Kaneka Easy DNA
335 Extraction Kit (Kaneka, Takasago, Japan). DNA extraction was followed by the PCR
336 analysis using an HIV *gag* primer set (sense: 5′-
337 AGTGGGGGGACATCAAGCAGCCATGCAAAT-3′, antisense: 5′-
338 TACTAGTAGTTCCTGCTATGTCACTTCC-3′) as described previously [47]. The
339 oligo DNAs were purchased from Sigma-Aldrich (Tokyo, Japan).
340
341 **Statistical analysis.** Statistical analysis was performed using GraphPad Prism
342 software version 7.0 (GraphPad Software, CA, USA). Statistical significance was
343 defined as $P < 0.05$. Comparisons between HIV-infected and uninfected samples were
344 performed using Wilcoxon's matched-pairs signed rank test, unless otherwise stated.
345 Multiple comparison analyses were done, if necessary, using Dunn's method.
346 Spearman's correlation coefficients were calculated for correlation analyses.
347
348

349

350 **References**

351 1 Parinitha, S. & Kulkarni, M. Haematological changes in HIV infection with
352 correlation to CD4 cell count. *Australas Med J* **5**, 157-162,
353 doi:10.4066/AMJ.20121008 (2012).

354 2 Corbeau, P. & Reynes, J. Immune reconstitution under antiretroviral
355 therapy: the new challenge in HIV-1 infection. *Blood* **117**, 5582-5590,
356 doi:10.1182/blood-2010-12-322453 (2011).

357 3 Blom, M., Epeldegui, M. & Uittenbogaart, C. H. in *HIV-Host Interactions*
358 (ed Theresa Li-Yun Chang) (InTech, 2011).

359 4 Ye, P., Kirschner, D. E. & Kourtis, A. P. The thymus during HIV disease:
360 role in pathogenesis and in immune recovery. *Curr HIV Res* **2**, 177-183 (2004).

361 5 Knutsen, A. P., Roodman, S. T., Freeman, J. J., Mueller, K. R. & Bouhasin,
362 J. D. Inhibition of thymopoiesis of CD34+ cell maturation by HIV-1 in an in vitro
363 CD34+ cell and thymic epithelial organ culture model. *Stem Cells* **17**, 327-338,
364 doi:10.1002/stem.170327 (1999).

365 6 Alexaki, A. & Wigdahl, B. HIV-1 infection of bone marrow hematopoietic
366 progenitor cells and their role in trafficking and viral dissemination. *PLoS Pathog* **4**,
367 e1000215, doi:10.1371/journal.ppat.1000215 (2008).

368 7 Dhurve, S. A. & Dhurve, A. S. Bone Marrow Abnormalities in HIV Disease.
369 *Mediterr J Hematol Infect Dis* **5**, e2013033, doi:10.4084/MJHID.2013.033 (2013).

370 8 Banda, N. K. *et al.* Depletion of CD34+ CD4+ cells in bone marrow from
371 HIV-1-infected individuals. *Biol Blood Marrow Transplant* **5**, 162-172,
372 doi:10.1053/bbmt.1999.v5.pm10392962 (1999).

373 9 Nakano, T., Kodama, H. & Honjo, T. Generation of lymphohematopoietic
374 cells from embryonic stem cells in culture. *Science* **265**, 1098-1101 (1994).

375 10 Schmitt, T. M. *et al.* Induction of T cell development and establishment of
376 T cell competence from embryonic stem cells differentiated in vitro. *Nat Immunol* **5**,
377 410-417, doi:10.1038/ni1055 (2004).
378 11 De Smedt, M., Hoebeke, I. & Plum, J. Human bone marrow CD34+
379 progenitor cells mature to T cells on OP9-DL1 stromal cell line without thymus
380 microenvironment. *Blood Cells Mol Dis* **33**, 227-232,
381 doi:10.1016/j.bcmd.2004.08.007 (2004).
382 12 Janas, M. L. *et al.* Thymic development beyond beta-selection requires
383 phosphatidylinositol 3-kinase activation by CXCR4. *J Exp Med* **207**, 247-261,
384 doi:10.1084/jem.20091430 (2010).
385 13 Mohtashami, M. *et al.* Direct comparison of Dll1- and Dll4-mediated Notch
386 activation levels shows differential lymphomyeloid lineage commitment outcomes. *J*
387 *Immunol* **185**, 867-876, doi:10.4049/jimmunol.1000782 (2010).
388 14 Weiss, R. A. HIV receptors and the pathogenesis of AIDS. *Science* **272**,
389 1885-1886 (1996).
390 15 Grivel, J. C. & Margolis, L. B. CCR5- and CXCR4-tropic HIV-1 are
391 equally cytopathic for their T-cell targets in human lymphoid tissue. *Nat Med* **5**,
392 344-346, doi:10.1038/6565 (1999).
393 16 Schnittman, S. M. *et al.* Preferential infection of CD4+ memory T cells by
394 human immunodeficiency virus type 1: evidence for a role in the selective T-cell
395 functional defects observed in infected individuals. *Proc Natl Acad Sci U S A* **87**,
396 6058-6062 (1990).
397 17 Okoye, A. A. & Picker, L. J. CD4(+) T-cell depletion in HIV infection:
398 mechanisms of immunological failure. *Immunol Rev* **254**, 54-64,
399 doi:10.1111/imr.12066 (2013).

400 18 Kucia, M. *et al.* CXCR4-SDF-1 signalling, locomotion, chemotaxis and
401 adhesion. *J Mol Histol* **35**, 233-245 (2004).
402 19 Lapidot, T. & Kollet, O. The essential roles of the chemokine SDF-1 and its
403 receptor CXCR4 in human stem cell homing and repopulation of transplanted
404 immune-deficient NOD/SCID and NOD/SCID/B2m(null) mice. *Leukemia* **16**, 1992-
405 2003, doi:10.1038/sj.leu.2402684 (2002).
406 20 Kucia, M. *et al.* Trafficking of normal stem cells and metastasis of cancer
407 stem cells involve similar mechanisms: pivotal role of the SDF-1-CXCR4 axis. *Stem*
408 *Cells* **23**, 879-894, doi:10.1634/stemcells.2004-0342 (2005).
409 21 Plotkin, J., Prockop, S. E., Lepique, A. & Petrie, H. T. Critical role for
410 CXCR4 signaling in progenitor localization and T cell differentiation in the
411 postnatal thymus. *J Immunol* **171**, 4521-4527 (2003).
412 22 Suzuki, H. *et al.* Intrathymic effect of acute pathogenic SHIV infection on
413 T-lineage cells in newborn macaques. *Microbiol Immunol* **49**, 667-679 (2005).
414 23 Marsden, M. D. *et al.* HIV latency in the humanized BLT mouse. *J Virol* **86**,
415 339-347, doi:10.1128/jvi.06366-11 (2012).
416 24 Dudek, T. E. & Allen, T. M. HIV-specific CD8(+) T-cell immunity in
417 humanized bone marrow-liver-thymus mice. *J Infect Dis* **208 Suppl 2**, S150-154,
418 doi:10.1093/infdis/jit320 (2013).
419 25 Pace, M. & O'Doherty, U. Hematopoietic stem cells and HIV infection. *J*
420 *Infect Dis* **207**, 1790-1792, doi:10.1093/infdis/jit120 (2013).
421 26 Tripathi, A. K., Misra, R., Kalra, P., Gupta, N. & Ahmad, R. Bone marrow
422 abnormalities in HIV disease. *J Assoc Physicians India* **53**, 705-710 (2005).
423 27 Hunt, P. W. *et al.* T cell activation is associated with lower CD4+ T cell
424 gains in human immunodeficiency virus-infected patients with sustained viral

425 suppression during antiretroviral therapy. *J Infect Dis* **187**, 1534-1543,
426 doi:10.1086/374786 (2003).
427 28 Isgro, A. *et al.* Altered clonogenic capability and stromal cell function
428 characterize bone marrow of HIV-infected subjects with low CD4+ T cell counts
429 despite viral suppression during HAART. *Clin Infect Dis* **46**, 1902-1910,
430 doi:10.1086/588480 (2008).
431 29 Shirozu, M. *et al.* Structure and chromosomal localization of the human
432 stromal cell-derived factor 1 (SDF1) gene. *Genomics* **28**, 495-500,
433 doi:10.1006/geno.1995.1180 (1995).
434 30 Moll, N. M. & Ransohoff, R. M. CXCL12 and CXCR4 in bone marrow
435 physiology. *Expert Rev Hematol* **3**, 315-322, doi:10.1586/ehm.10.16 (2010).
436 31 Petrie, H. T. Cell migration and the control of post-natal T-cell
437 lymphopoiesis in the thymus. *Nat Rev Immunol* **3**, 859-866, doi:10.1038/nri1223
438 (2003).
439 32 Nixon, C. C. *et al.* HIV-1 infection of hematopoietic progenitor cells in vivo
440 in humanized mice. *Blood* **122**, 2195-2204, doi:10.1182/blood-2013-04-496950
441 (2013).
442 33 Carter, C. C. *et al.* HIV-1 utilizes the CXCR4 chemokine receptor to infect
443 multipotent hematopoietic stem and progenitor cells. *Cell Host Microbe* **9**, 223-234,
444 doi:10.1016/j.chom.2011.02.005 (2011).
445 34 Ho Tsong Fang, R., Colantonio, A. D. & Uittenbogaart, C. H. The role of
446 the thymus in HIV infection: a 10 year perspective. *AIDS* **22**, 171-184,
447 doi:10.1097/QAD.0b013e3282f2589b (2008).

448 35 Bordoni, V. *et al.* Early ART in primary HIV infection may also preserve
449 lymphopoiesis capability in circulating haematopoietic progenitor cells: a case report.
450 *J Antimicrob Chemother*, doi:10.1093/jac/dku559 (2015).
451 36 Akkina, R. New insights into HIV impact on hematopoiesis. *Blood* **122**,
452 2144-2146, doi:10.1182/blood-2013-08-518274 (2013).
453 37 Hoebeke, I. *et al.* T-, B- and NK-lymphoid, but not myeloid cells arise from
454 human CD34(+)CD38(-)CD7(+) common lymphoid progenitors expressing
455 lymphoid-specific genes. *Leukemia* **21**, 311-319, doi:10.1038/sj.leu.2404488 (2007).
456 38 Bordoni, V. *et al.* Bone Marrow CD34+ Progenitor Cells from HIV-
457 Infected Patients Show an Impaired T Cell Differentiation Potential Related to
458 Proinflammatory Cytokines. *AIDS Res Hum Retroviruses* **33**, 590-596,
459 doi:10.1089/aid.2016.0195 (2017).
460 39 Savkovic, B. *et al.* A quantitative comparison of anti-HIV gene therapy
461 delivered to hematopoietic stem cells versus CD4+ T cells. *PLoS Comput Biol* **10**,
462 e1003681, doi:10.1371/journal.pcbi.1003681 (2014).
463 40 Liu, Y., Zhou, J., Pan, J. A., Mabiala, P. & Guo, D. A novel approach to
464 block HIV-1 coreceptor CXCR4 in non-toxic manner. *Mol Biotechnol* **56**, 890-902,
465 doi:10.1007/s12033-014-9768-7 (2014).
466 41 Suzuki, K., Ahlenstiel, C., Marks, K. & Kelleher, A. D. Promoter Targeting
467 RNAs: Unexpected Contributors to the Control of HIV-1 Transcription. *Mol Ther*
468 *Nucleic Acids* **4**, e222, doi:10.1038/mtna.2014.67 (2015).
469 42 Costin, J. M. Cytopathic mechanisms of HIV-1. *Virol J* **4**, 100,
470 doi:10.1186/1743-422x-4-100 (2007).
471 43 Tsukamoto, T., Yamamoto, H., Okada, S. & Matano, T. Recursion-based
472 depletion of human immunodeficiency virus-specific naive CD4(+) T cells may

473 facilitate persistent viral replication and chronic viraemia leading to acquired
474 immunodeficiency syndrome. *Med Hypotheses* **94**, 81-85,
475 doi:10.1016/j.mehy.2016.06.024 (2016).
476 44 Adachi, A. *et al.* Production of acquired immunodeficiency syndrome-
477 associated retrovirus in human and nonhuman cells transfected with an infectious
478 molecular clone. *J Virol* **59**, 284-291 (1986).
479 45 Holmes, R. & Zuniga-Pflucker, J. C. The OP9-DL1 system: generation of
480 T-lymphocytes from embryonic or hematopoietic stem cells in vitro. *Cold Spring*
481 *Harb Protoc* **2009**, pdb.prot5156, doi:10.1101/pdb.prot5156 (2009).
482 46 Tsukamoto, T. & Okada, S. The use of RetroNectin in studies requiring in
483 vitro HIV-1 infection of human hematopoietic stem/progenitor cells. *J Virol*
484 *Methods* **248**, 234-237, doi:10.1016/j.jviromet.2017.08.003 (2017).
485 47 Suzuki, K. *et al.* Prolonged transcriptional silencing and CpG methylation
486 induced by siRNAs targeted to the HIV-1 promoter region. *J RNAi Gene Silencing* **1**,
487 66-78 (2005).
488
489

490 **Acknowledgements**

491

492 We thank Drs. Kazuo Matsui and Shoichi Kawakami of Fukuda Hospital,
493 Kumamoto, Japan for their assistance with cord blood sampling. This work was
494 supported by the National Health and Medical Research Council, Australia (project
495 grant). It was also partially supported by grants from the following organizations: the
496 Japan Agency for Medical Research and Development (Research program on
497 HIV/AIDS, No. 16fk0410108h0001); Ministry of Education, Culture, Sports, Science
498 and Technology, Japan (Grants-in-Aid for Science Research, No. 25114711) and
499 Kumamoto University (AIDS International Collaborative Research Grant). We thank
500 Enago (www.enago.jp) for the English language review.

501

502

503 **Author information**

504

505 The authors declare no competing financial interests associated with the present
506 work. Correspondence and requests for materials should be addressed to
507 ttsukamoto@med.kindai.ac.jp.

508

509
510 **Figures**
511

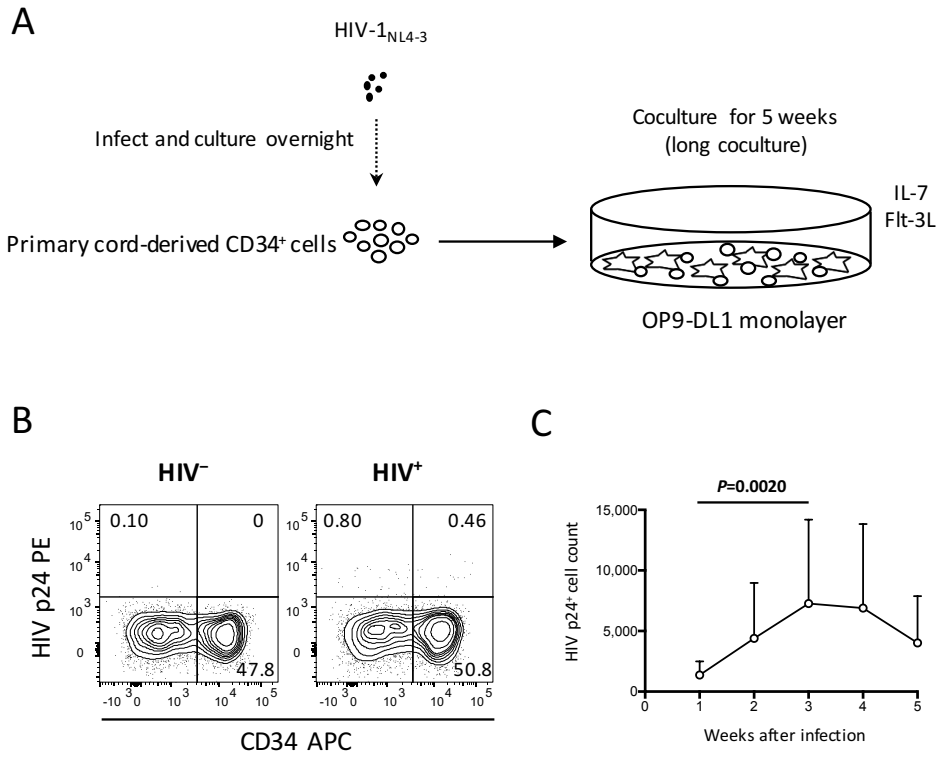

512
513
514 **Figure 1.** Primary umbilical cord-derived CD34$^+$ cells are susceptible to HIV
515 infection. Coculture of HIV-infected primary cord-derived CD34$^+$ cells with OP9-
516 DL1 cells resulted in persistent viral replication for 5 weeks (n = 12). (A) Schematic
517 representation of experiment 1 (long coculture). Cord-derived CD34$^+$ cells were
518 infected with HIV-1$_{NL4-3}$ and cocultured with OP9-DL1 cells for 5 weeks. (B)
519 Intracellular HIV p24 expression was tested 1 week after infection. HIV p24$^+$ cells
520 were found in both the CD34$^+$ and CD34$^-$ fractions of HIV-infected samples.
521 Representative plots are shown. (C) HIV p24$^+$ cell counts at weeks 1–5 post-infection
522 (n = 12). Statistical analyses were performed using the Wilcoxon matched-pairs
523 signed rank test.
524

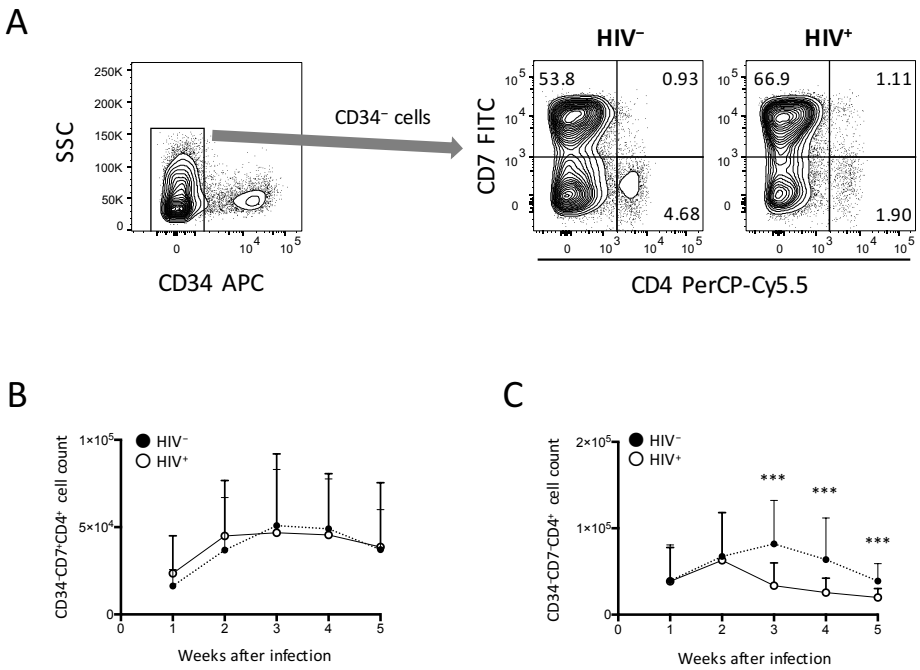

525
526
527 **Figure 2.** Pre-exposure of primary cord-derived CD34$^+$ cells to HIV-1 affected the
528 dynamics of OP9-DL1 cocultured cells (n = 12). (A) Representative plots showing the
529 loss of CD34$^-$CD7$^-$CD4$^+$ cells in the HIV-infected cocultures 3–5 weeks after
530 infection. (B-C) Cell counts were compared between HIV$^+$ and HIV$^-$ cocultures for
531 (B) CD34$^-$CD7$^+$CD4$^+$ and (C) CD34$^-$CD7$^-$CD4$^+$ cells. Statistical analyses were
532 performed using the Wilcoxon matched-pairs signed rank test. ***: $P < 0.001$.
533

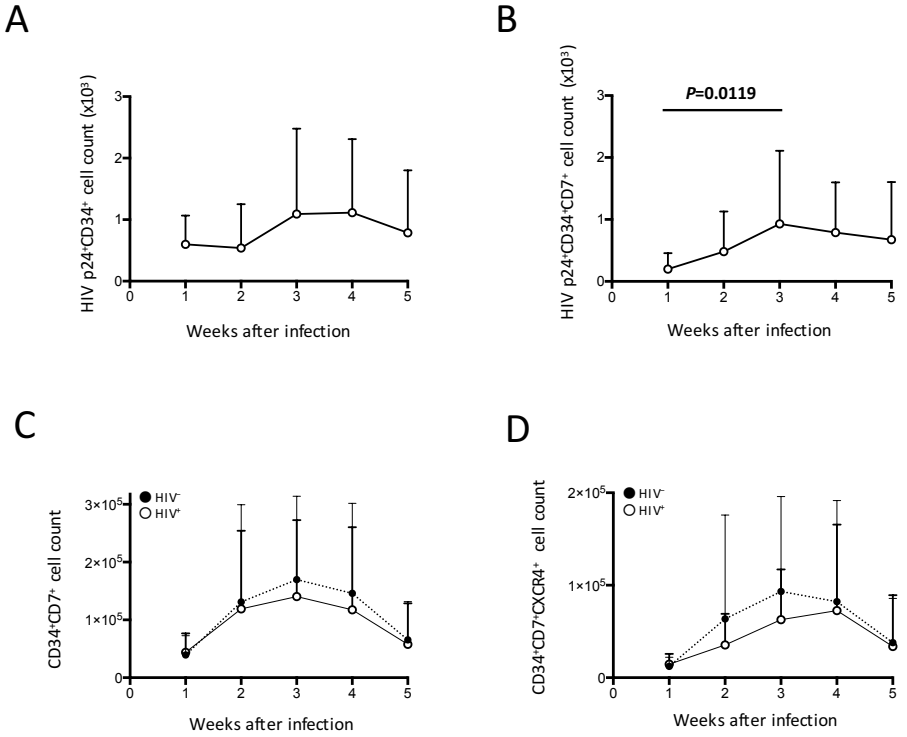

534

535 **Figure 3.** Pre-exposure of primary cord-derived $CD34^+$ cells to HIV-1 affected the
536 dynamics of $CD34^+$ cells in the subsequent OP9-DL1 cocultures (n = 12). (A) HIV
537 $p24^+CD34^+$ cell counts in HIV^+ OP9-DL1 cocultures. (B) HIV $p24^+CD34^+CD7^+$ cell
538 counts in HIV^+ OP9-DL1 cocultures. (C–D) Cell counts were compared between
539 HIV^+ and HIV^- cocultures for (C) $CD34^+CD7^+$ and (D) $CD34^+CD7^+CXCR4^+$ cells.
540 Statistical analyses were performed using the Wilcoxon matched-pairs signed rank
541 test.

542

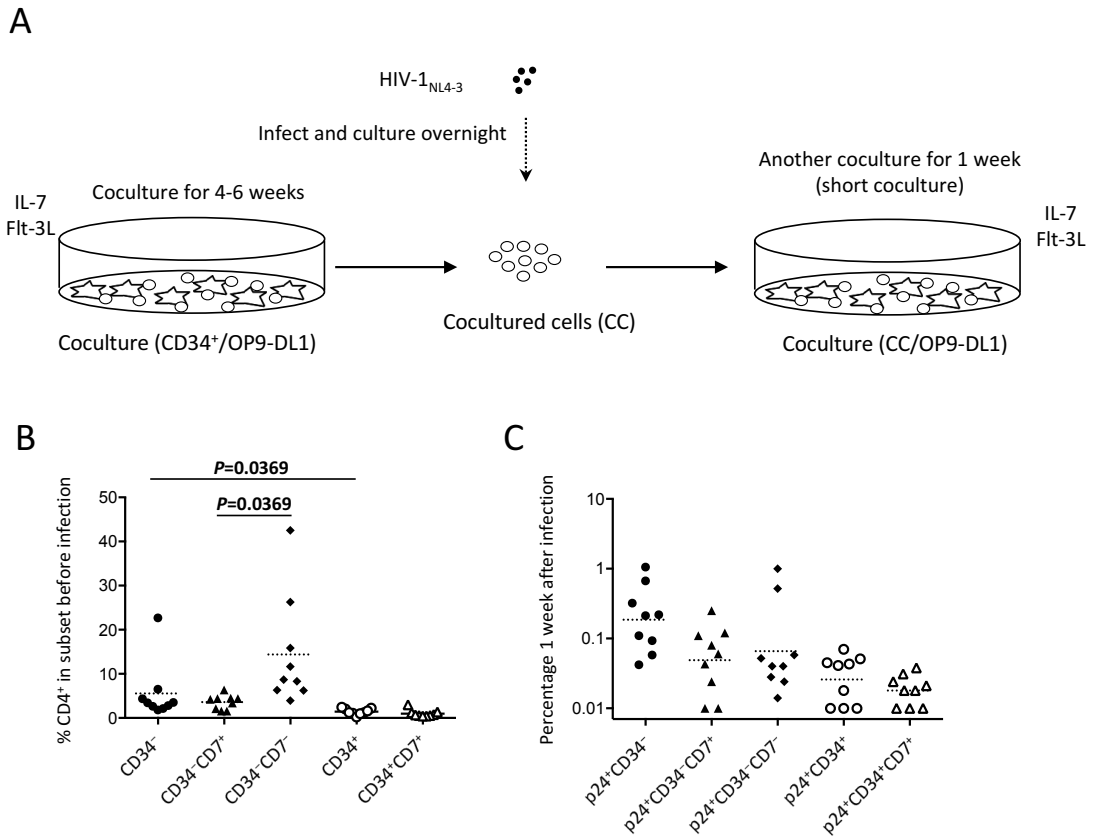

Figure 4. Experiment 2 (short coculture, n = 9) was performed to further analyse the dynamics of $CD34^+$ cells in the presence of HIV-1. (A) Schematic representation of experiment 2 (short coculture). Primary cord-derived $CD34^+$ cells were cocultured with OP9-DL1 cells for 4–6 weeks. Cells were then collected and infected with HIV-1_{NL4-3}. The infected cells were cocultured again with OP9-DL1 cells for 1 week, collected and analysed. (B) Percentages of $CD4^+$ cells in $CD34^-$, $CD34^-CD7^+$, $CD34^-CD7^-$, $CD34^+$ and $CD34^+CD7^+$ subsets before infection. A multiple comparison test was performed to compare $CD34^-$ and $CD34^+$ cells or $CD34^-CD7^+$ and $CD34^-CD7^-$ cells. (C) Frequencies of HIV $p24^+$, $p24^+CD34^-CD7^+$, $p24^+CD34^-CD7^-$, $p24^+CD34^+$ and $p24^+CD34^+CD7^+$ cells measured 1 week after the second post-infection coculture (n = 9). Statistical analysis was performed using the multiple comparison test with Dunn's method.

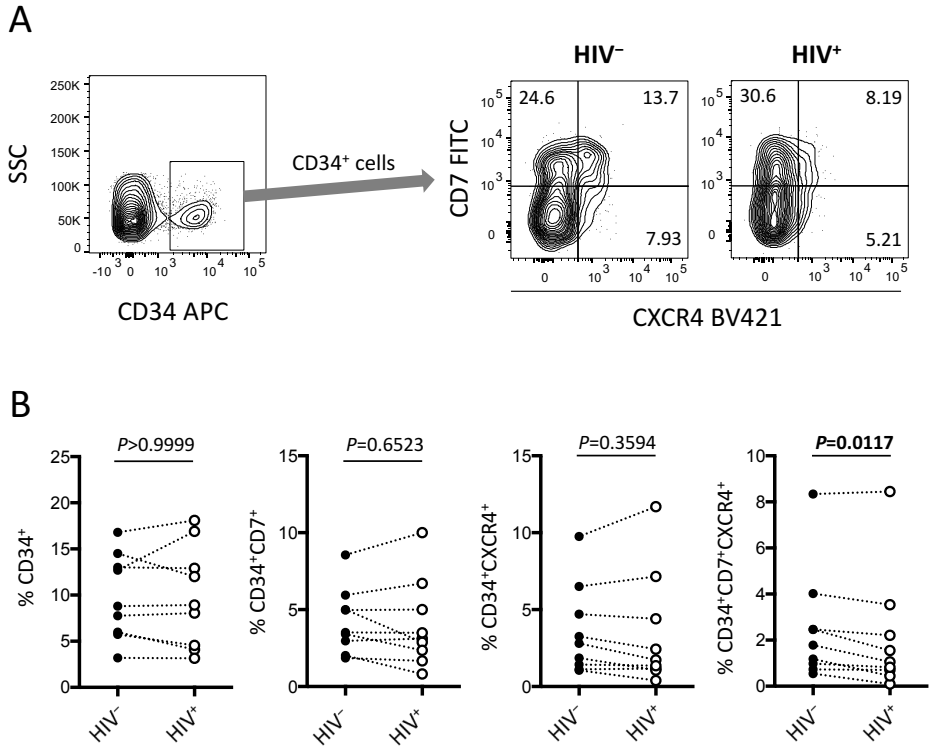

557

558 **Figure 5.** CD34$^+$ cells in experiment 2 (short coculture, n = 9) were analysed 1 week
559 after the second post-infection coculture. (A) Representative plots showing
560 CD7/CXCR4 expression levels in CD34$^+$ cells. An HIV$^+$ sample is compared to its
561 autologous uninfected counterpart. (B) Frequencies of CD34$^+$ (left), CD34$^+$CD7$^+$
562 (middle left), CD34$^+$CXCR4$^+$ (middle right) and CD34$^+$CD7$^+$CXCR4$^+$ (right) cells
563 were compared between HIV$^+$ and HIV$^-$ samples. Statistical analyses were performed
564 using the Wilcoxon matched-pairs signed rank test.

565

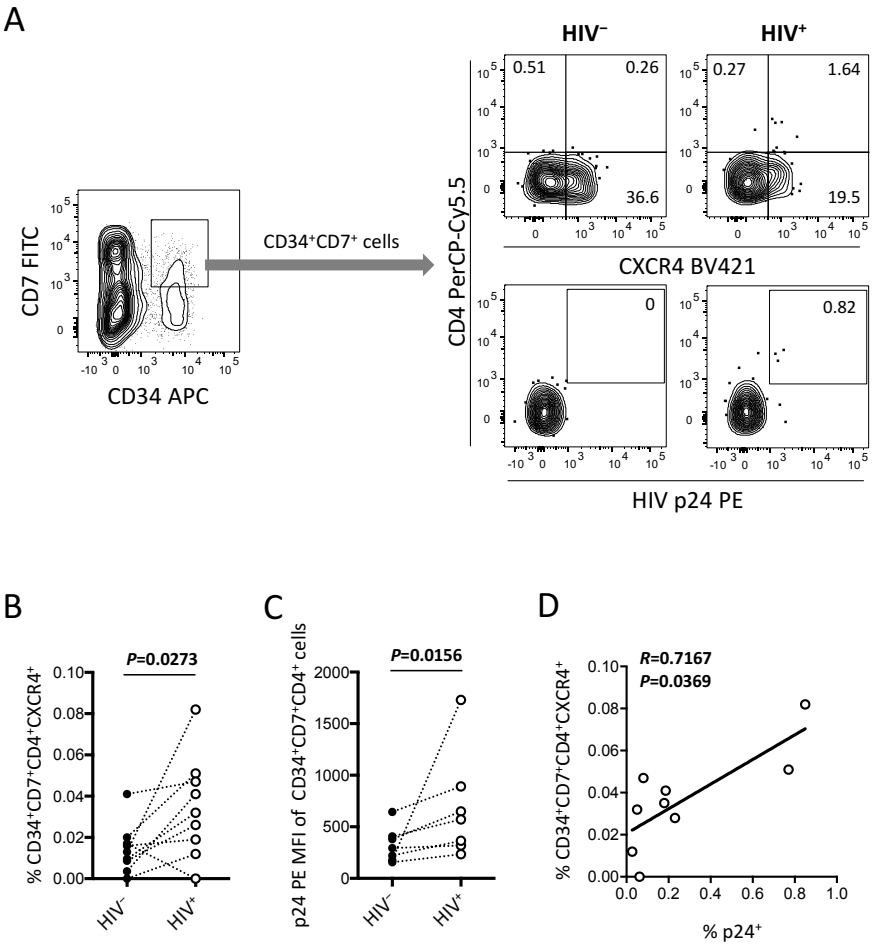

Figure 6. $CD34^+CD7^+$ cells in experiment 2 (short coculture, n = 9) were analysed 1 week after the second post-infection coculture. For these analyses, compensation matrices were checked carefully to exclude false-positive events. (A) Representative plots showing CD4/CXCR4 and CD4/p24 expression levels in $CD34^+CD7^+$ cells. An HIV^+ sample is compared to its autologous uninfected counterpart. (B) Comparison of the frequencies of $CD34^+CD7^+CD4^+CXCR4^+$ cells between HIV^+ and HIV^- samples. (C) p24 mean fluorescence intensities (MFIs) of $CD34^+CD7^+CD4^+$ cells were compared between HIV^+ and HIV^- samples (n = 7). (D) The frequencies of $CD34^+CD7^+CD4^+CXCR4^+$ cells were correlated with those of $p24^+$ cells. Comparisons were performed using the Wilcoxon matched-pairs signed rank test. Spearman's correlation coefficient was calculated for the correlation analysis.

578 **Extended Data figures and tables**
579

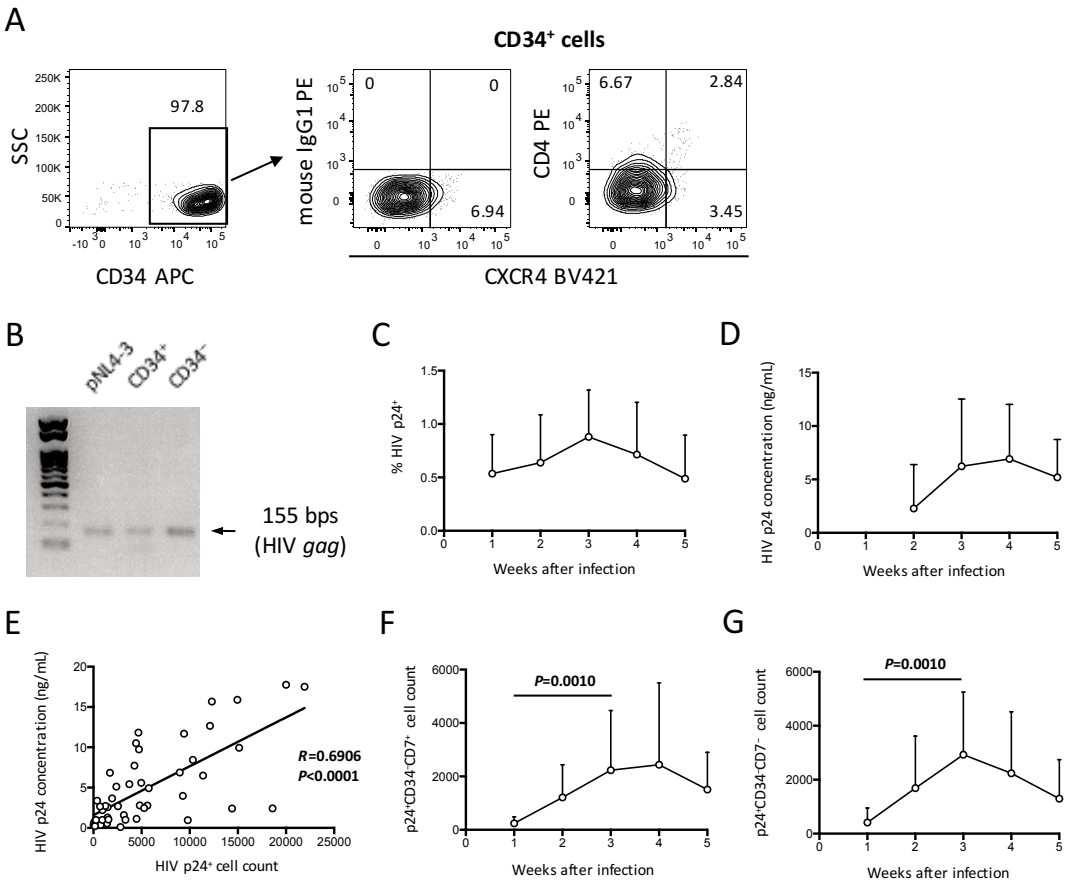

580

581 **Extended Data Figure 1.** HIV infection of cord-derived CD34$^+$ cells and derivatives
582 were evaluated. (A) Primary cord-derived CD34$^+$ cells were gated and tested for CD4
583 and CXCR4 expression by flow cytometry. Representative plots are shown. The CD4
584 signal levels were compared to the signal levels of a PE-conjugated mouse isotype
585 control antibody. (B) The CD34$^+$ and CD34$^-$ fractions of an HIV-infected sample
586 were separated using the CD34 microbead method. Total DNA was isolated and
587 analysed by PCR. HIV gag DNA was detected in both the CD34$^+$ and CD34$^-$
588 fractions. A PCR sample using the HIV molecular plasmid pNL4-3 was used as a
589 control. (C) Percentage of HIV p24$^+$ cells in HIV$^+$ OP9-DL1 coculture samples tested
590 weekly by intracellular staining and flow cytometry. (D) Coculture supernatants of
591 HIV-infected samples were tested for HIV p24 concentrations by ELISA at weeks 2–
592 5. (E) Correlation analysis between the frequencies of HIV p24$^+$ cells and HIV p24
593 concentrations. The weeks 2–5 data in F and G are included (n = 48). Spearman's
594 correlation coefficients are shown. (F) p24$^+$CD34$^-$CD7$^+$ cell counts. (G)
595 p24$^+$CD34$^-$CD7$^-$ cell counts. Comparisons were performed using the Wilcoxon
596 matched-pairs signed rank test.

597

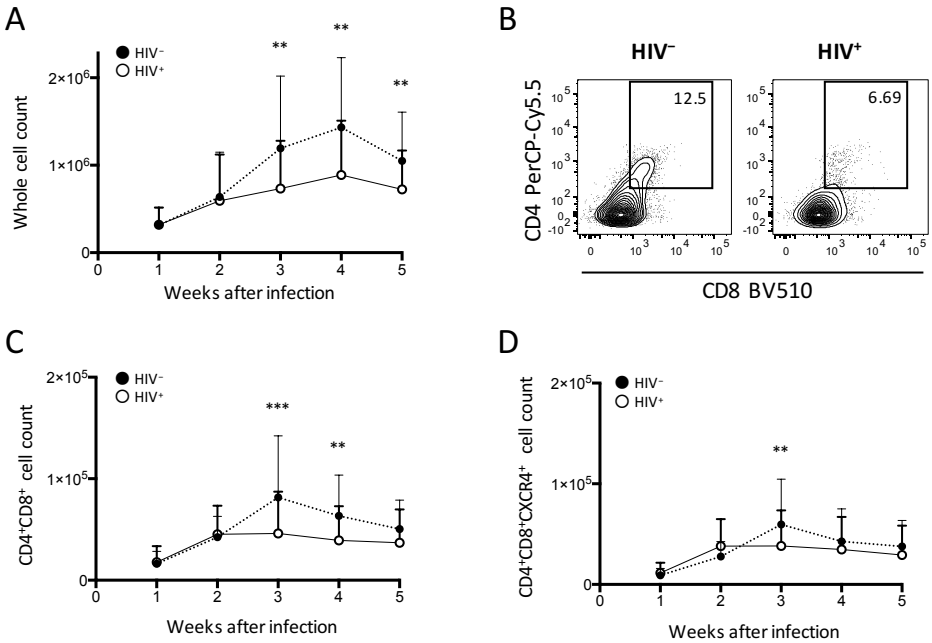

598

599 **Extended Data Figure 2.** Pre-exposure of primary cord-derived $CD34^+$ cells to HIV-
600 1 affected the dynamics of OP9-DL1 cocultured cells. (A) Whole cell counts were
601 compared between HIV^+ and HIV^- cocultures. (B) Representative plots for samples
602 displaying reduced frequencies of $CD4^+CD8^+$ cells 3–5 weeks after HIV pre-exposure
603 of primary $CD34^+$ cells and coculture. The plots were selected from week 4 samples.
604 (C–D) Cell counts were compared between HIV^+ and HIV^- cocultures for (C)
605 $CD4^+CD8^+$ and (D) $CD4^+CD8^+CXCR4^+$ cells. Statistical analyses were performed
606 using the Wilcoxon matched-pairs signed rank test. **: $P < 0.01$, ***: $P < 0.001$.
607

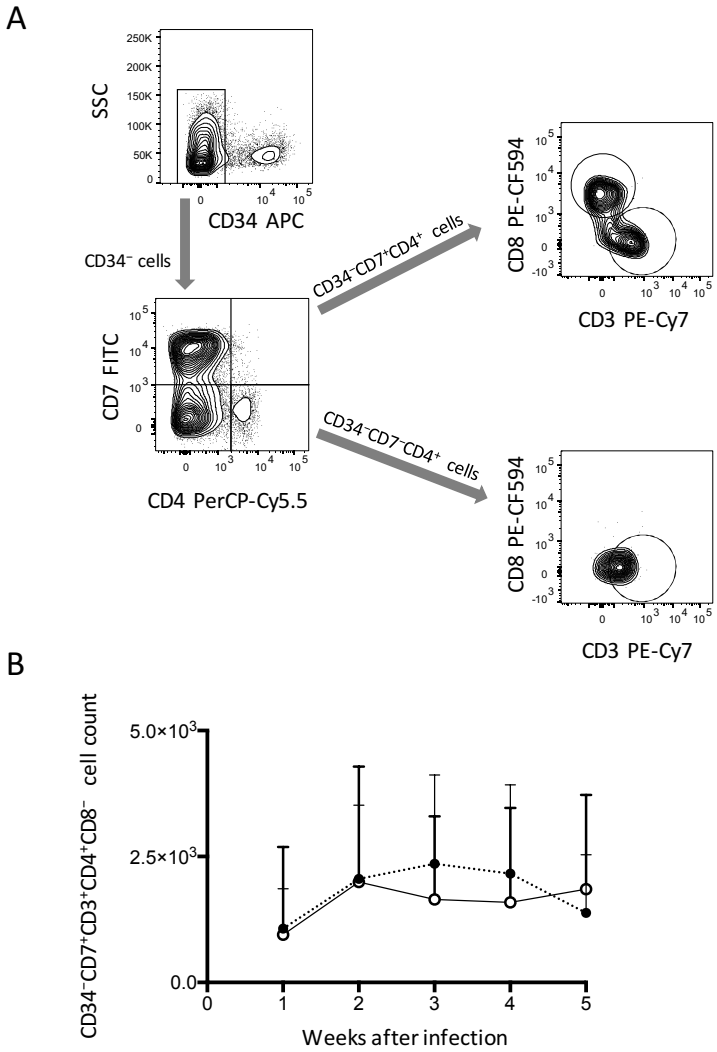

608
609
610 **Extended Data Figure 3.** Analysis of $CD34^{-}CD4^{+}$ cells. (A) Flow cytometry plots
611 showing the phenotype analysis of $CD34^{-}CD4^{+}$ cells in an OP9-DL1 coculture.
612 Representative plots are shown. Cord-derived $CD34^{+}$ cells were cocultured with OP9-
613 DL1 cells for 4 weeks. Cells were collected and analysed by flow cytometry. $CD34^{-}$
614 cells were gated by CD7 and CD4 expression. $CD7^{+}CD4^{+}$ and $CD7^{-}CD4^{+}$ cells were
615 further gated by CD8 and CD3 expression. The analysis revealed that $CD7^{+}CD4^{+}$
616 cells contained different subsets including $CD3^{-}CD4^{+}CD8^{+}$ and $CD3^{+}CD4^{+}CD8^{-}$
617 cells, whereas $CD7^{-}CD4^{+}$ cells were mostly $CD3^{+}CD4^{+}CD8^{-}$ cells. These results
618 indicate that CD4/CD8 double-positive thymocytes, $CD7^{+}$ CD4 T cells and $CD7^{-}$
619 CD4 T cells were generated via coculture of cord-derived $CD34^{+}$ and OP9-DL1 cells.
620 (B) $CD34^{-}CD7^{+}CD3^{+}CD4^{+}CD8^{-}$ cell counts.

621

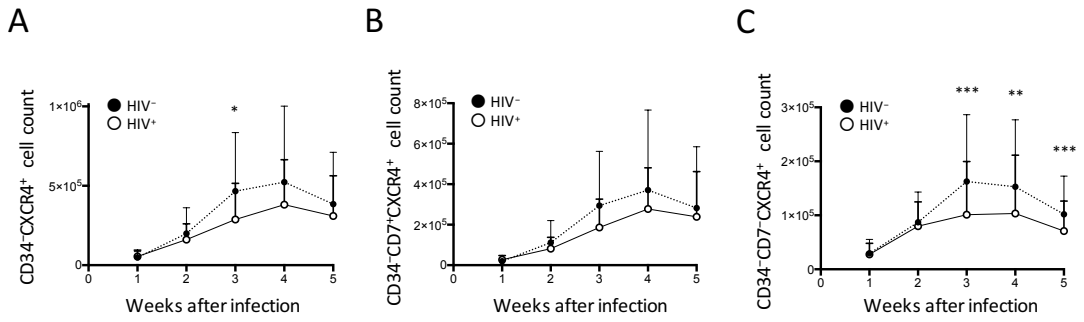

622 **Extended Data Figure 4.** Phenotypes of $CD34^-$ cells in the OP9-DL1 cocultures
623 were analysed weekly for 5 weeks after HIV-1 infection. Cell counts were compared
624 with those in uninfected samples. (A) $CD34^-CXCR4^+$ cell counts. (B)
625 $CD34^-CD7^+CXCR4^+$ cell counts. (C) $CD34^-CD7^-CXCR4^+$ cell counts. Comparisons
626 were performed using the Wilcoxon matched-pairs signed rank test. *: $P < 0.05$, **: P
627 < 0.01, ***: $P < 0.001$.
628

629

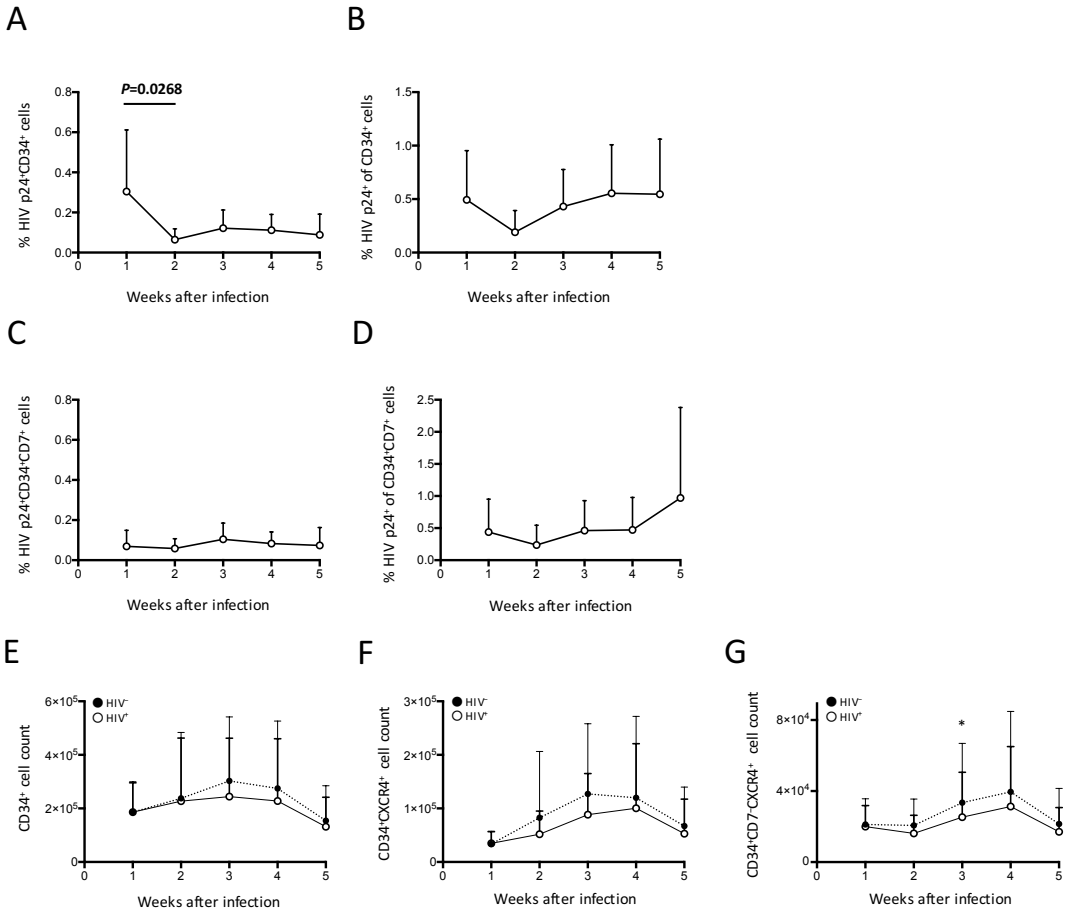

630
631

632 **Extended Data Figure 5.** (A–D) HIV p24^{+} subset dynamics were analysed. (A)
633 Percent p24^{+}CD34^{+} cells. (B) Percent p24^{+} cells among CD34^{+} cells. (C) Percent
634 p24^{+}CD34^{+}CD7^{+} cells. (D) Percent p24^{+} cells among CD34^{+}CD7^{+} cells. (E–G)
635 CD34^{+} subset dynamics were analysed and compared between HIV^{+} and HIV^{-}
636 samples. (E) CD34^{+} cell counts. (F) CD34^{+}CXCR4^{+} cell counts. (G)
637 CD34^{+}CD7^{-}CXCR4^{+} cell counts.

638

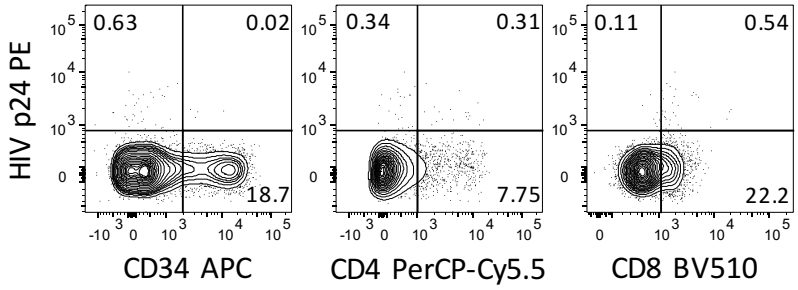

Extended Data Figure 6. Experiment 2 (short coculture, n = 9) was performed to further analyse the dynamics of $CD34^+$ cells in the presence of HIV-1. Representative plots showing HIV $p24^+$ cells 1 week after infection. The majority of $p24^+$ cells were $CD34^-$ (left). HIV replication may be causing CD4 downregulation (middle). Frequencies of $CD8^+$ cells in $p24^+$ cells were variable among the samples (right).

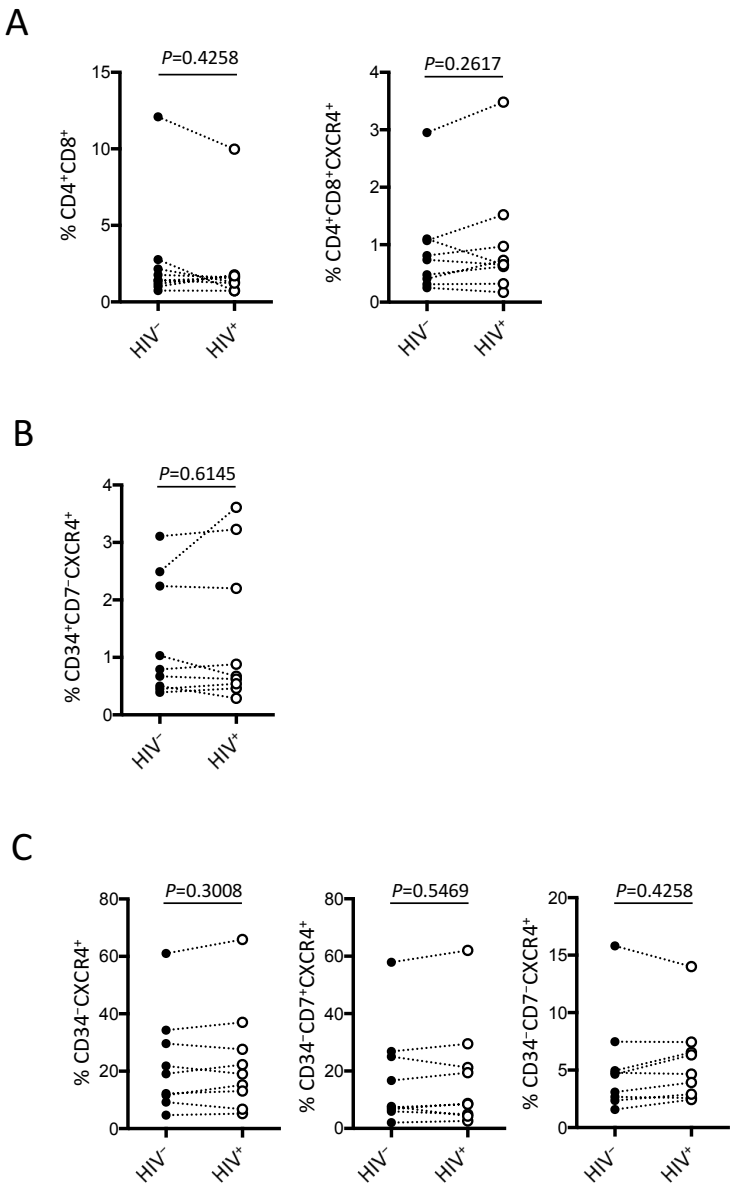

647
648
649 **Extended Data Figure 7.** The frequencies of subsets were compared between HIV-
650 infected and uninfected samples 1 week after infection. (A) $CD4^{+}CD8^{+}$ cells. (B)
651 $CD4^{+}CD8^{+}CXCR4^{+}$ cells. (C) $CD34^{-}CXCR4^{+}$ (left), $CD34^{-}CD7^{+}CXCR4^{+}$ (middle)
652 and $CD34^{-}CD7^{-}CXCR4^{+}$ (right) cells. Comparisons were performed using the
653 Wilcoxon matched-pairs signed rank test.
654

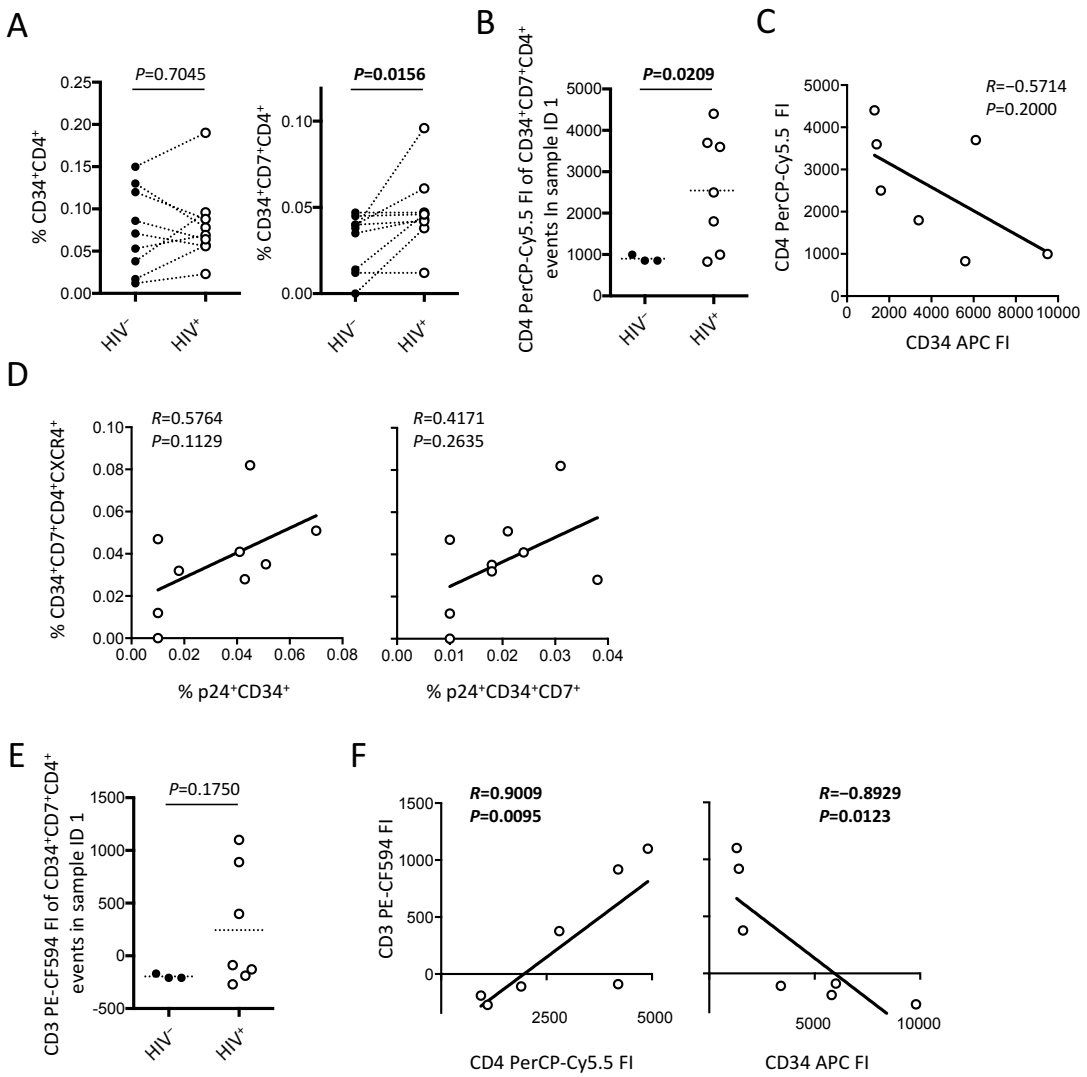

Extended Data Figure 8. $CD34^+CD7^+CD4^+$ cells were further analysed. (A) Comparison of $CD34^+CD4^+$ (left) and $CD34^+CD7^+CD4^+$ (right) frequencies between HIV^+ and HIV^- samples. (B) Fluorescence intensities (FIs) of $CD34^+CD7^+CD4^+$ cells were compared between HIV^+ and HIV-$^-$ samples using the Mann-Whitney test. (C) Correlation between the CD4 and CD34 FI of $CD34^+CD7^+CD4^+$ cells in the HIV^+ sample of ID 1 were analysed (n = 3 for HIV^-; n = 7 for HIV^+). (D) $CD34^+CD7^+CD4^+CXCR4^+$ cells were tested for correlations with the frequencies of $p24^+CD34^+$ (left) and $p24^+CD34^+CD7^+$ (right) cells. (E) Comparison of CD3 FIs between HIV-infected and uninfected samples. (F) Correlation analysis between CD3 FIs and CD4 (left) or CD34 (right) FIs. Comparisons were made using the Wilcoxon matched-pairs signed rank test unless otherwise noted. Spearman's correlation coefficients were calculated for correlation analyses.

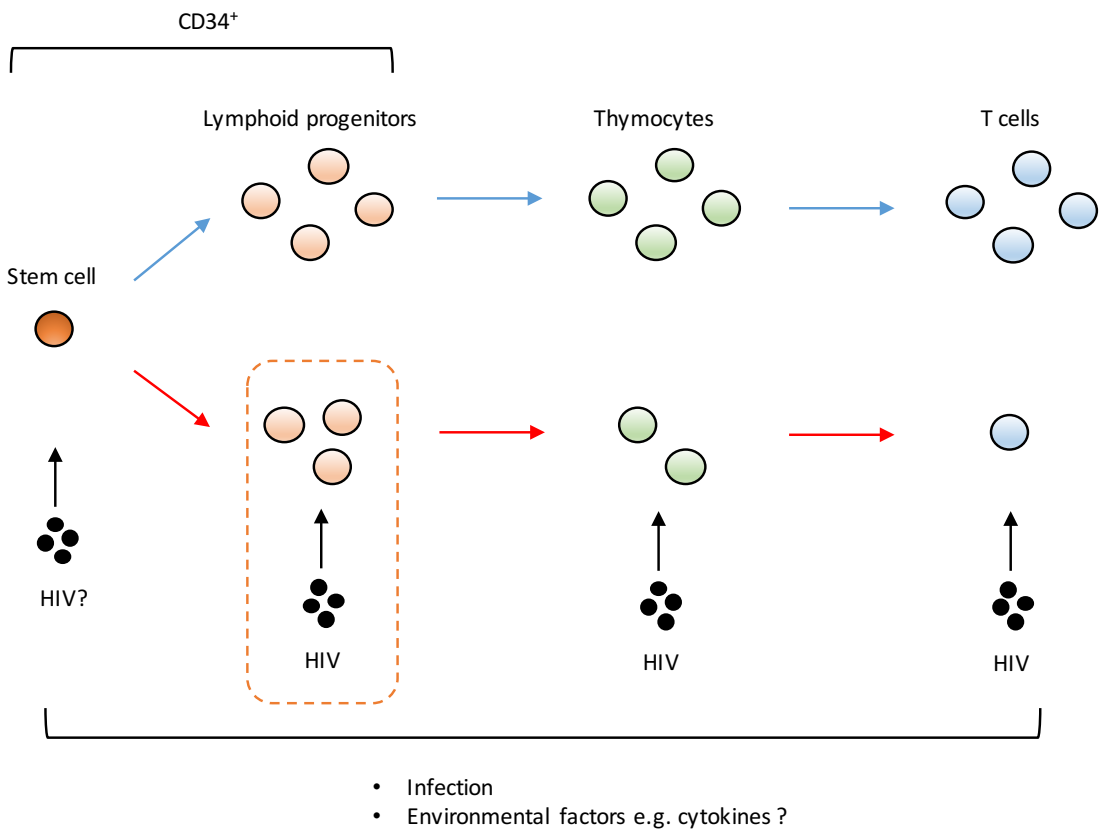

Extended Data Figure 9. A schematic representation of factors potentially influencing the decrement of $CD4^+$ T cells. Thymocytes and T cells are highly susceptible to HIV infection. However, the decrease of $CD34^+$ lymphoid progenitor counts occurs early and precedes the decrease of thymocyte and T-cell counts. Although the mechanisms for the decrease of $CD34^+$ lymphoid progenitors are unclear, this decline may limit the production of thymocytes and T cells.

679

Subset	Cell count in infected samples (mean ± SD, n = 4)	% in the mean whole cell count
Whole	390,000 ± 155,000	100
$p24^+$	547 ± 258	0.140
$p24^+CD34^-CD7^+$	326 ± 242	0.084
$p24^+CD34^-CD7^-$	124 ± 56	0.032
$p24^+CD34^+$	97 ± 42	0.025
$p24^+CD34^+CD7^+$	80 ± 31	0.021

680
681 **Extended Data Table 1.** Mean cell counts (n = 4) in different HIV $p24^+$ subsets of
682 OP9-DL1-cocultured cells. The whole cell count data were obtained with 4/9 samples
683 of experiment 2 (short coculture, Figs. 4-6, Extended Data Figs. 4-5), in which cord-
684 derived $CD34^+$ cells were first cocultured with OP9-DL1 for 4-6 weeks, infected with
685 HIV-1_{NL4-3}, cocultured again for 1 week, and analysed by flow cytometry. The
686 percentages in the mean whole cell count are also shown and comparable to Fig 4C
687 SD: standard deviation.

688
689

690

Subset	Cell count (mean ± SD, n = 4)		$\% \frac{(infected-uninfected)}{uninfected}$
	uninfected	*infected*	
Whole	400,000 ± 169,000	390,000 ± 155,000	−2.5
$CD4^+CD8^+$	5,790 ± 3,510	4,920 ± 2,360	**−15.0**
$CD4^+CD8^+CXCR4^+$	3,290 ± 1,760	3,050 ± 1,840	−7.3
$CD34^+$	32,900 ± 18,200	32,100 ± 21,400	−2.3
$CD34^+CD7^+$	16,700 ± 9,500	16,100 ± 12,100	−3.6
$CD34^+CXCR4^+$	18,300 ± 11,000	18,300 ± 14,700	−0.1
$CD34^+CD7^+CXCR4^+$	12,100 ± 7,800	11,900 ± 11,100	−2.0
$CD34^+CD7^-CXCR4^+$	6,150 ± 3,870	6,380 ± 3,990	+3.7
$CD34^+CD7^+CD4^+$	129 ± 42	178 ± 74	**+38.0**
$CD34^-CXCR4^+$	149,000 ± 164,000	157,000 ± 167,000	+5.8
$CD34^-CD7^+CXCR4^+$	131,000 ± 161,000	139,000 ± 162,000	+5.6
$CD34^-CD7^-CXCR4^+$	16,900 ± 7,500	18,000 ± 8,000	+7.8

691

692 **Extended Data Table 2.** Mean cell counts (n = 4) in different subsets of OP9-DL1
693 cocultured cells. The whole cell count data were obtained with 4/9 samples of
694 experiment 2 (short coculture, Figs. 4-6, Extended Data Figs. 4-5), in which cord-
695 derived $CD34^+$ cells were first cocultured with OP9-DL1 for 4-6 weeks, infected with
696 HIV-1_{NL4-3}, cocultured again for 1 week, and analysed by flow cytometry. Cell counts
697 in HIV-infected samples were compared with uninfected control samples. Percent
698 changes of the subset cell counts by HIV infection were calculated and shown in the
699 right column. Percent changes > 10% or < −10% are shown in bold. SD: standard
700 deviation.

701
702